Environmental Science Processes & Impacts

PAPER

View Article Online
View Journal

Cite this: DOI: 10.1039/d4em00124a

Bubble-mediated generation of airborne nanoplastic particles†

Eva Rosendal Kjærgaard, Freja Hasager, Sarah Suda Petters, ‡ Marianne Glasius and Merete Bilde *

Received 8th March 2024
Accepted 10th June 2024

DOI: 10.1039/d4em00124a

rsc.li/espi

Micro- and nanoplastic particles have been detected in most environmental compartments. The presence of microplastics in the remote marine atmosphere and close to large lakes suggests bubble mediated water–air transfer as a source of airborne microplastics, however, quantitative estimates of plastic emission from surface waters remain uncertain. In this work, we elucidate the emission of submicron polystyrene nanospheres by bubble bursting in a laboratory setting from low salinity waters (salinity 0–1.0 g kg^{-1}), polystyrene particle diameter (103, 147 and 269 nm), aqueous particle number concentrations in the range 4×10^7–2×10^9 cm^{-3}, and bubble formation rate (0.88–3.35 L min^{-1} of air). Production of polystyrene aerosols was demonstrated using a scanning mobility particle sizer and confirmed by analysis of filter samples using pyrolysis gas chromatography coupled to mass spectrometry. We show that production of polystyrene aerosol particles scales linearly with the number concentration of plastic particles in the water. Our results suggest that small amounts (0.01 g kg^{-1}) of salt increase polystyrene particle production. To the best of our knowledge this is the first study of bubble mediated water–air transfer of plastic particles as small as 100 nm.

Environmental significance

It has recently become clear that plastic particles constitute a pollutant in the atmosphere with largely unknown impacts on human health, eco-systems and climate. Nano- and microplastic accumulates in ocean and freshwater reservoirs. This work addresses transfer of plastic nanoparticles from low-saline waters to air *via* bubble bursting at the water/air interface and contributes to the emerging understanding of transfer of nanoplastics from polluted surface waters to the atmosphere.

Introduction

Plastic pollution in the form of microplastic (MP, 1 μm–5 mm)[1] and nanoplastic (NP, < 1 μm)[1] is accumulating in most environmental compartments on Earth[2] including soil,[3] oceans,[2] and fresh water.[4] Micro- and nanoplastics are emitted directly into the environment or formed as a result of weathering processes of plastic debris from, for example, cleaning and skincare products, pharmaceuticals, textiles, and tire wear.[5,6] In recent years, it has become clear that plastic is also a pollutant in the atmosphere and that the atmosphere may act as an efficient and fast transfer medium for microplastic.[7,8] Several methods are being developed for identifying and quantifying nano- and microplastic in complex atmospheric aerosol mixtures.[9–12] Airborne plastic may be inhaled with potentially highly adverse, albeit not yet fully resolved, effects on respiratory human health.[13] Airborne micro- and nanoplastics may also affect global climate by serving as seeds for cloud droplet[14] and ice crystal[15] formation and by directly affecting the radiative balance.[16]

The transfer of MP and NP from surface waters has recently been proposed as a source of plastic in the atmosphere.[1,14] Field work support this hypothesis: Allen *et al.*[14] detected microplastic in marine boundary layer air in samples dominated by sea spray and Trainic *et al.*[17] detected polyethylene and polypropylene microplastic using μ-Raman analysis in both air and water in the North Atlantic Ocean suggesting local production of marine microplastics *via* wave breaking. There is large variation in the proposed source strengths ranging from ~800 ton yr^{-1} (ref. 18) to 8.6×10^6 ton yr^{-1}.[19] More recently, lakes and lake spray aerosol (LSA) have been receiving much attention. Lakes are often located near populated areas and can be

Department of Chemistry, Aarhus University, DK-8000 Aarhus C, Denmark. E-mail: bilde@chem.au.dk

† Electronic supplementary information (ESI) available: Experimental details on set-up and chemicals used, AEGOR headspace equilibration calculation, details on integration of particle spectra, filter sampling details, experimental time evolution of PSL number concentration, SMPS transfer function calculation, full SMPS size spectra, and test of reproducibility. See DOI: https://doi.org/10.1039/d4em00124a

‡ Current address: Center for Environmental Research and Technology, University of California, Riverside, 92507 California, USA.

hotspots for pollution.[20,21] May *et al.*[22] measured particles from SSA and LSA at a rural site >25 km from the nearest Great Lakes sources and found that LSA contributed to the total PM mass during a day-long wind event.

Number and mass concentrations of microplastic in surface waters are typically quantified for sizes larger than around 300 micrometer[23] and little is known about concentrations of smaller particle sizes although number concentrations of these are expected to be greater.[21] In the North Atlantic subtropical gyre surface water concentrations of up to 1.62 particles per m^3 (D_p > 335 μm) of surface water were observed.[24] Recently, Materić *et al.*[25] reported polystyrene (PS) nanoplastic concentrations of 4.2 μg L^{-1} (upper diameter of 200 nm) corresponding to minimum 10^{12} nanoplastic particles per m^3 of water in the Dutch Wadden sea.

Recently, it has become clear that concentrations of microplastic in freshwater systems can be of similar magnitude or even larger than in subtropical oceanic gyres.[21] Egessa *et al.*[26] report concentrations in the range of 0.02–2.19 microplastic particles m^{-3} (size range 0.3–4.9 mm) for coastal surface waters in northern Lake Victoria in East Africa, which is the second largest fresh water lake in the world.[26] High concentrations of microplastic have also been measured in several large Chinese lakes.[27,28] For example, Su *et al.*[28] report concentrations of 3.4–25.8 × 10^3 plastic particles m^{-3} (>333 μm) in surface waters of the third largest freshwater lake in China, Taihu Lake. In the US, Mason *et al.*[29] sampled plastic in Lake Michigan and report surface concentrations of plastic of ∼17 000 particles km^{-2} (>333 μm). This converts to ∼0.1 particles m^{-3} assuming the height of the surface layer to be 16 cm corresponding to the height of the used Mantra trawl opening. To our knowledge, the number concentrations of particles smaller than 333 μm have not been reported in lakes. In lack of such knowledge, we estimate the number concentration of 100 nm particles by scaling the lower and upper number concentrations listed above by the diameter ratio cubed. We here assume spherical particles and a volume concentration and density of the 100 nm particles equal to that of the larger particles (assuming a diameter of 333 μm). On this basis, number concentration of 100 nm particles would be in the range 4 × 10^9–1 × 10^{15} particles per m^3 across these lakes. We expect these values to represent upper limits, but field measurements are needed to establish the number concentrations of nanoplastic particles in lakes.

Lately, and during the course of this work, laboratory studies have confirmed transfer of plastic from water to air in bubble bursting processes for particle of size 300 nm and larger.[18,30–35] Bubble bursting has been studied from waters ranging from fresh to saline and air entrainment has been mimicked in different ways. Most studies have addressed particles made of polystyrene (PS), polypropylene (PP) and polyethylene (PE) which are among the plastic polymers produced in the highest amount[36] and identified in both sea[37] and lake[21] water. As highlighted above, freshwater lakes can contain high concentrations of plastic debris with number concentrations of MP particles that can exceed those in oceanic gyres. Even so, to our knowledge few laboratory studies have so far addressed transfer of microplastic from freshwater to air.

Masry *et al.*[34] bubbled air through a diffuser (sintered glass frit) into 4 L of water and detected transfer of particles in the size range 250 nm–32 μm using an optical particle counter and demonstrated transfer of PS particles of diameters 350 nm, 600 nm and 1 μm from pure water. They observed a higher transfer of particles when the surfactant Sodium Dodecyl Sulfate (SDS) was added to the water. For PE particles (size distribution from 200 to 9900 nm) no transfer was observed unless the particles had been UV aged.

Oehlsclägel *et al.*[31] use a stainless steel frit to generate bubbles into 1 L deionized water and quantified polystyrene particle transfer for sizes between 0.35–2 μm using an optical particle counter. Number concentrations in water were around 10^{11} particles per L. They observed a size dependent transfer with a maximum for particle sizes of 1 μm.

Harb *et al.*[30] deployed a Marine Aerosol Reference Tank (MART) generating bubbles by plunging sheet of water into a water pool of 147 L of artificial seawater (salinity of 35 g kg^{-1}, room temperature). Harb *et al.* demonstrated and quantified transfer of PS (diameters of 0.5, 2 and 10 μm) and PE particles (size distribution ranging from 1 to 10 μm) at different concentrations ranging from 10–10^5 L^{-1} for PS and 10^7–10^8 L^{-1} for PE particles in the water (10^4–10^8 m^{-3}). Aerosolization was observed to increase monotonically with increasing number concentration of plastic particles in the water. The aerosolization factor (defined as the number concentration of plastic particles in the air relative to the number concentration in the water) was the same for 0.5 and 2 μm PS particles and significantly lower for 10 μm particles. Consistent with Masry *et al.*[34] transfer of PE was observed to be less efficient than for PS.

Catarino *et al.*[32] used an intermittent water jet (mini-MART tank, water volume of 6 L) to investigate the transfer of fluorescent PS particles (0.5, 1, 5 and 10 μm in diameter, respectively) in artificial seawater (salinity 31 g kg^{-1}) at a temperature of 18 °C for a constant concentration of plastic particles in the water of 10^9 m^{-3}. They report transfer of all particle sizes from water to air with an increase in number with decreasing particle size consistent with the trend reported by Harb *et al.*[30]

Shui *et al.*[33] used a diffuser setup (130 mL of water) with varying salinity (0, 17 and 34 psu) and fluorescent PS particles with a diameter of 1.04 μm. The concentration of PS particles in the water was 2.3 × 10^8 particles m^{-3}. Two experiments were also performed with addition of alginic acid sodium salts from brown algae. Shiu *et al.*[33] confirm transfer of MPs in both fresh and salt water and observed that the number of transferred plastic particles increased with increasing salinity. Furthermore, transfer of PS particles was increased with addition of the alginic acid sodium salts to the saline solutions, but not when added to fresh water.

Yang *et al.*[18] studied transfer of PS (0.4, 0.6, 0.8, 1.0, and 1.6 μm in diameter), PE and PP particles (10, 20, 70 and 700 μm in diameter) from artificial sea water (3.5% NaCl) and in natural seawater using a plunging jet. Concentrations in the water of 0.8 μm PS particles was up to 0.5 g m^{-3} which corresponds to 1.8 × 10^{12} particles m^{-3} of water if a PS density of 1.05 g cm^{-3} is assumed.

Finally, while the studies mentioned above have deployed bubble plumes, Shaw *et al.*[35] demonstrated and quantified transfer of PE particles in the size range of 10 to 280 μm (diameter) in a single bubble system. Here bubbles escape from a needle and ascend in liquids with different densities (deionized water, artificial seawater with a salinity of 42 g kg^{-1} and ethanol), all with a small amount of the surfactant SDS added.

Typically, marine sea spray[38–40] and lake spray[41,42] aerosol size distributions have main modes of dry particle diameters below 300 nm, however as seen from the list above, little knowledge is available on the transfer of particles smaller than 400 nm in size from sea as well as fresh water.

In the current work, we complement existing knowledge about the bubble-mediated transfer of NP across the air–water interface under conditions with salinities up to 1.0 g kg^{-1} We use the AEGOR tank[38] with bubble generation by a diffuser at the bottom of the tank and perform characterization of particle size at high resolution using a scanning mobility particle sizer and confirm chemical composition using detailed off-line chemical analysis. We use monodisperse polystyrene particles (103, 147 and 269 nm) and investigate effects of NP concentration in the water, bubble formation rate and low salinity on the plastic particle transfer from water to air for concentrations of NPs in the range 4×10^7–2×10^9 particles per cm^3 of water.

Materials and methods

Materials

Polystyrene latex spheres of 103 ± 1 nm diameter from Bangs Laboratories, Inc. (NT05N) and 147 ± 3 nm and 269 ± 5 nm diameter from Thermo Scientific™ (3000 Series Nanosphere™) were all aqueous suspension of 1% solids by mass with a density of 1.05 g mL^{-1} at 25 °C. The flasks were ultrasonicated for 10 s prior to measurements to ensure particle dispersion. The following salts (with purities) were purchased from Sigma Aldrich: NaCl (≥99.5%), $MgCl_2 \cdot 6H_2O$ (≥99.0%), $CaCl_2 \cdot 2H_2O$ (≥99.5%), KNO_3 (≥99.5%), NaBr (≥99.0%), K_2SO_4 (≥99.0%) and Na_2SO_4 (≥99.0%). Milli-Q water (EMD Millipore, >18.2 MΩ·cm resistivity at 25 °C, 2 ppb TOC) was used in all experiments. Synthetic salt water composed of Cl^-, Na^+, SO_4^{2-}, K^+, Ca^{2+}, Br^-, Mg^{2+}, and NO_3^- with mass contributions relative to Cl^- of 1, 0.56, 0.14, 1.7×10^{-2}, 2.2×10^{-2}, 3.1×10^{-3}, 6.8×10^{-2}, and 2.6×10^{-3}, respectively, was prepared following Nielsen and Bilde[43] and diluted to salinities ranging from 0.01 to 1.0 g kg^{-1} (Table S1†). Dry particle-free air was obtained from the in-house clean air system and routed through an additional inline air purification system (TSI 3074B) before use.

Experimental setup

The AEGOR sea spray simulation tank[38] at Aarhus University was used to generate aerosols by bubble bursting at the water surface. A schematic of the setup is shown in Fig. S1.† Briefly, the AEGOR tank is a 34 L temperature-controlled stainless steel cylindric container with ports for sampling from the headspace and temperature probes both in the air and water. The temperature in the tank is regulated by continuous flow of coolant (glycol–water mixture) inside the double walled system of the tank. The temperature of the coolant, tank water, tank headspace and room temperature are continuously measured with Vernier temperature probes. The tank is filled with 20 L of solution and the height of the water column is 29 cm. In this study air bubbles were generated using a sintered glass diffuser at the bottom of the tank (40 mm diameter, VitraPOR sintered glass filters, Cat.-Nr. 15054, ISO 4793-80, Por. 4, pore-diameter 10–16 μm, ROBU Glasfilter-Geraete GmbH, Germany). All airflows were controlled with thermal mass flow controllers (Vögtlin Instruments) and measured in-line with a TSI 4100 series flowmeter. Air purified using a filtered air supply was bubbled through the diffuser at the bottom of the tank. AEGOR was operated with a sweep airflow through the headspace of 5.6 L min^{-1} and a flowrate of 3.35 L min^{-1} through the diffuser as the base case. Assuming well-mixed air in the headspace and the stated flows (see Section S1.3†), the time to reach 95% of the equilibrium particle concentration in the 13.9 L headspace of AEGOR is 4.7 min.

Aerosols were sampled from the headspace, dried using two silica diffusion dryers to a relative humidity below 25% (measured in-line after the dryers with Rotronic HygroFlex5), and routed to downstream instrumentation. The efflorescence relative humidity is 48% for NaCl,[44] ∼50% for artificial sea salt (Sigma Seasalt),[45] and ∼45% for an Atlantic Ocean sea water sample.[44] We thus assume that the particles sampled from the headspace are dry when measured in the SMPS. The particle-laden air was sampled through conductive silicone tubing to reduce electrostatic particle loss. We cannot exclude some particle loss to walls in the AEGOR tank and tubing enroute to the SMPS. As in other studies *e.g.* ref. 30,46 such losses are not accounted for in the analysis in this study.

Dry particle size distributions were measured online using a scanning mobility particle sizer (SMPS; TSI 3082) and an optical particle sizer (OPS; TSI 3330). The SMPS consisted of a differential mobility analyzer (DMA; TSI 3081) coupled to a condensation particle counter (CPC; TSI 3750). Prior to the DMA, particles passed through an X-ray charge neutralizer (TSI 3088) and an impactor (orifice 0.0701 cm, with an average upper D50 of 709 nm). The SMPS sampled with a sheath flow of 5 L min^{-1} and a sample flow of 1.08 L min^{-1}, reporting a size spectrum (9.9–538 nm, 223 bins, 128 channels per decade) every 5.5 min (300 s voltage scans with a 30 s flush time). The AIM 11.3.0 software was used for data-acquisition and inversion, including corrections for multiple charges and diffusion loss in the DMA. When possible, log-normal fits were applied to peaks in the size distribution to obtain particle number concentrations (cm^{-3}; see Section S2†). The OPS sampled at 1 L min^{-1}, reporting size spectra (0.3–10 μm, 16 bins) every 60 s. The AIM 10.3 software was used without a refractive index correction.

In some experiments, after completion of measurements using the SMPS, particles were sampled directly from the AEGOR headspace during bubbling onto quartz fiber filters (Frisenette, 47 mm, pre-baked at 600 °C for 6 h) using a custom-built metal filter holder. Sampling was conducted overnight for 14 or 21 h, without diffusion dryers, at a continuous flow of 1.6 or 2.9 L min^{-1}, respectively. Flow was controlled by an SKC Flite

3 pump (model 901-3011); other instrumentation was disconnected from the tank during filter sampling. A procedural blank filter was obtained to determine contamination from the experimental procedure and sample preparation. The filter samples were placed in a closed glass container at −18 °C until analysis by pyrolysis gas chromatography coupled to mass spectrometry (py-GC-MS). The pyrolysis module (GERSTEL PYRO) was interfaced with a gas chromatograph coupled to a mass spectrometer (Agilent Technologies 7890b and 5977a). Details on filter sampling and analysis are given in Section S3† and details on the polystyrene analysis method are given by Hasager *et al.*[9]

Experiments

Table 1 provides an overview of the experiments performed, listing the operating conditions, instruments, and aqueous solution composition. Before and after each experiment the empty tank interior was wiped with a paper towel and ethanol, then filled with a mixture of 200 mL 96% ethanol and 20 L demineralized water and purged with clean air flowing through the diffuser and headspace for at least 30 min. This was then repeated with 20 L of Milli-Q water.

Each experiment started with 20 L of Milli-Q water in the clean tank. The tank was closed and purged with clean air flowing through the diffuser and headspace for approximately 15 min. After this, background particle size spectra, generated by bubbling the Milli-Q water, were recorded by the SMPS and OPS for at least 30 min. Then, polystyrene latex (PSL) solution was added to the Milli-Q water through a small port in the tank lid with no bubbling (for 103 nm PSL experiments the PSL was weighed in a glass beaker and then added to the tank while the diffuser was off). For saltwater experiments the salt was added after the addition of PSL. Before each new measurement, the system was allowed at least 15 min to reach stable particle concentration in the headspace (the system equilibrated rapidly, as demonstrated in Section S4†). The temperature was kept constant at 20 °C during all experiments.

Results and discussion

Transfer of nanoplastics from pure water

Fig. 1 shows size distributions of dried aerosol from the headspace of AEGOR before and after addition of PSL particles to Milli-Q water. Results are summarized in Table 2 and details of peak integration are given in the ESI, Section S2.† After addition of either 103, 147 or 269 nm PSL particles we clearly observe a peak of corresponding diameter in the headspace of AEGOR. As an example, after addition of 147 nm PSL particles (Fig. 1B) we observe a peak centered at 145 nm (median diameter) with an integrated particle number concentration of 13 cm^{-3}. The peak is slightly broader than predicted from the standard deviation of the PSL size (±3 nm), which is explained by the width of the DMA transfer function (see Section S5†). The production flux of particles is 1.9×10^3 particles per second, calculated following Christiansen *et al.*[38] as the integrated particle number concentration obtained by the SMPS (N_{air}) multiplied by the sum of the sweep air flow through the headspace and the diffuser flowrate.

The particle production at diameters consistent with those of the added PSL particles, demonstrates aerosolization of PSL particles *via* bubble bursting at the air–water interface. This was further established by off-line chemical analysis of aerosols collected onto filters. Aerosol particle filter collection and py-

Table 1 List of experiments. All experiments were performed in the AEGOR tank at 20 °C with 20 L of (initially pure) Milli-Q water. PSL refers to polystyrene latex solution

#	Date	Water composition	Salinity (g kg^{-1})	Diffuser flow (L min^{-1})	Instrumentation
1	17.05.22	25 drops 147 nm PSL	—	3.35	SMPS, OPS
2	18.05.22	50 drops 147 nm PSL [a]	—	3.35	SMPS
3a	19.05.22	25 drops 147 nm PSL, variation of	—	3.35	SMPS
3b		diffuser flowrate		2.60	
3c				1.74	
3d				0.88	
4	20.05.22	25 drops 269 nm PSL	—	3.35	SMPS
5	23–25.05.22	25 drops 147 nm PSL + sea salt	0	3.35	SMPS, HTDMA-AMS[b]
5a			0.01		
5b			0.02		
5c			0.05		
5d			0.1		
5e			0.2		
6a	21–23.03.23	103 nm PSL, 5 drops	—	3.35	SMPS, OPS
6b		10 drops [c]			
6c		20 drops			
6d		30 drops			
6e		40 drops			
6f		50 drops			

[a] 25 additional drops added to previous 20 L sample from May 17. [b] A companion paper addresses hygroscopicity of the transferred particles. For further details see Petters *et al.*[10] [c] Drops of PSL spheres (103 nm) were added consecutively. The number given is the total number added.

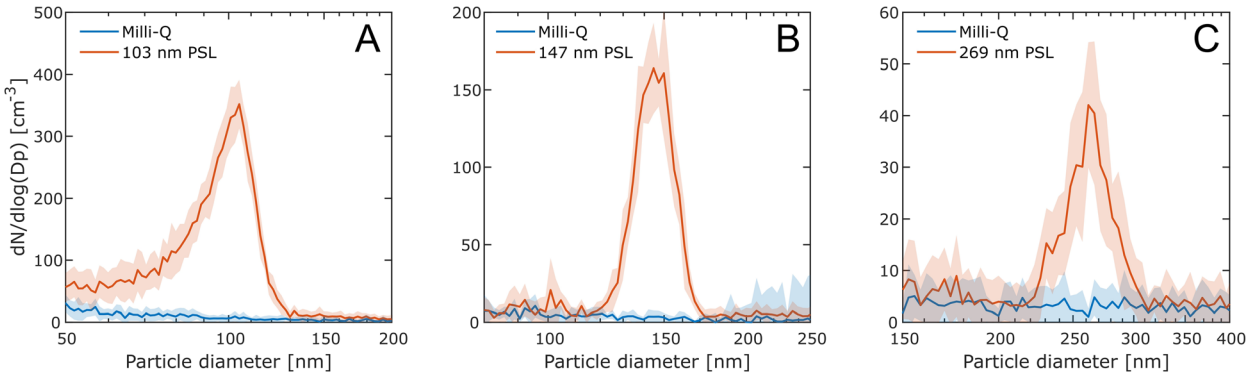

Fig. 1 Mean particle number size distribution measured by the SMPS (headspace air) for a solution of Milli-Q water (blue) and after addition of PSL (orange). (A) Addition of 30 drops of 103 nm PSL (Experiment 6 in Table 1). (B) Addition of 25 drops of 147 nm PSL (Experiment 1). (C) Addition of 25 drops of 269 nm PSL (Experiment 4). The diffuser flowrate was 3.35 L min^{-1} and the temperature was held constant at 20 °C. All data are averages of 30 min (5 scans) and 1 standard deviation is shown as a shading. Note the different *y*-axes and logarithmic *x*-axes in the different panels. For the full-size spectrum down to 10 nm see ESI Section S6.†

GC-MS analysis was performed for experiments 2, 4 and 5d and the chemical analysis unambiguously confirms the presence of PSL in the air sampled from the AEGOR headspace (Section S3†). Recently, Chen *et al.*[11] have measured microplastics, including polystyrene, in urban air samples also using py-GC-MS.

The number of larger particles (>300 nm) as observed by the OPS was negligible (Fig. S8†) and no peaks appeared in the size spectra observed by the SMPS above the peak of PSL (Section S6†). These observations give rise to the conclusion that formation of particles by coagulation or agglomeration of PSL particles either does not happen under the conditions in the AEGOR tank or are such that agglomerated particles are not transferred from water to air. This is in contrast to Masry *et al.*[34] who report water–air transfer of agglomerates of PSL spheres from aerosolization of 350 nm particles from Milli-Q water.

Table 2 Results of experiments listed in Table 1. *N* is number concentration, *M* is mass concentration, D_p is particle diameter, N_w is the estimated concentration of polystyrene latex (PSL) particles in water, N_{air} is the integrated PSL number concentration in air, and N_{flux} is the particle water–air flux per second. For simplicity errors are only shown for N_{air}. Since aerosol number concentrations are typically provided in number of particles per cm^3 of air, number concentrations are here given per cm^3 of water or air. The number concentrations in water fall in the range 4×10^7–2×10^9 cm^{-3} corresponding to 4×10^{10}–2×10^{12} L^{-1} or 4×10^{13}–2×10^{15} m^{-3} of water

	PSL in water			PSL in air (SMPS)			
#	D_p (nm)	N_w[a] (cm^{-3})	M_w[a] (g m^{-3})	D_p[b] (nm)	N_{air}[b] (cm^{-3})	M_{air}[c] (μg m^{-3})	N_{flux}[d] (particles s^{-1})
1	147 ± 3	2.6×10^8	0.45	145	13 ± 2	0.02	1.9×10^3
2	147 ± 3	5.2×10^8	0.91	145	30 ± 1	0.05	4.5×10^3
3a (3.35 L min^{-1})				145	13 ± 1	0.02	1.9×10^3
3b (2.60 L min^{-1})	147 ± 3	2.6×10^8	0.45	144	5.6 ± 1	0.01	7.7×10^2
3c (1.74 L min^{-1})				144	2.1 ± 1	0.004	2.6×10^2
3d (0.88 L min^{-1})				145	1.4 ± 2	0.002	1.5×10^2
4	269 ± 5	4.2×10^7	0.45	262	3.0	0.03	4.5×10^2
5 (0 g kg^{-1})				143	10 ± 1	0.02	1.6×10^3
5a (0.01 g kg^{-1})				144	25 ± 2	0.04	3.7×10^3
5b (0.02 g kg^{-1})	147 ± 3	2.6×10^8	0.45	144	23 ± 1	0.04	3.4×10^3
5c (0.05 g kg^{-1})				144	23 ± 1	0.04	3.4×10^3
5d (0.1 g kg^{-1})				145	29 ± 1	0.05	4.3×10^3
5e (0.2 g kg^{-1})				147	41	0.07	6.1×10^3
6a	103 ± 1	1.7×10^8	0.10	—	13	0.007	2.3×10^3
6b	103 ± 1	3.0×10^8	0.18	—	19	0.01	3.5×10^3
6c	103 ± 1	6.5×10^8	0.39	98	31 ± 2	0.02	5.7×10^3
6d	103 ± 1	1.0×10^9	0.60	98	45 ± 2	0.03	8.1×10^3
6e	103 ± 1	1.3×10^9	0.81	98	57 ± 1	0.03	1.0×10^4
6f	103 ± 1	1.7×10^9	1.02	98	72 ± 3	0.04	1.3×10^4

[a] Calculation based on the density of PSL particles (1.05 g cm^{-3}) and average mass of 1 droplet PSL solution 0.0363 ± 0.0013 g for 147 nm, $n = 6$. For 103 nm PSL total added volume in each experiment was weighed, for 269 nm same droplet mass as for 147 nm was assumed. 1% solids by mass, and assuming spherical particles. [b] Median diameter and number concentration (N_{air}) derived from log-normal fits to distributions, if possible, see Section S2 for details. Errors represent the standard deviation on integration of each distribution within the average. [c] M_{air} calculated from N_{air} based on the density of PSL particles (1.05 g cm^{-3}), D_p (103, 147 or 269 nm) and assuming spherical particles. [d] Obtained by $N_{air} \times Q_{headspace}$ (where $Q_{headspace}$ = diffuser flowrate + sweep air flowrate). For comparison the notation in Harb *et al.*[30] is $E = C_{out} \times Q_{out}$.

While we use a sintered glass filter with pore size 10–16 μm, Masry *et al.* use a porosity grade 3 filter (16–40 μm pore size) and a wire mesh with a 125 μm mesh size. The air flowrate through the diffuser is higher in this study compared to Masry *et al.*, 3.35 *vs.* 2.5 L min^{-1}, respectively. Additionally, the water column height in this study is 29 cm whereas it is 13 cm in Masry *et al.* It is however not clear if these differences can explain the difference between our results and those of Masry *et al.* and the conditions favoring or preventing transfer of agglomerates should be further investigated.

Similarly to Sofieva *et al.*,[47] we observe a background signal of small particles (diameter mostly <60 nm) from bubbling of air through Milli-Q water. In most cases the number of the smallest particles increases after addition of PSL, as observed in Fig. S6a.† These changes likely arise from additives in the PSL solution. Reproducibility was confirmed by the comparison of experiments 1, 3 and 5, which were performed using the same concentrations of 147 nm PSL particles in Milli-Q water and diffuser flow rate of 3.35 L min^{-1} (see Table 2 and Fig. S9†). The three experiments were performed on different days with emptying, cleaning and refilling of the tank in between. Based on the particle fluxes given in Table 2 and the time of the individual experiments the loss of particles from the water never exceeded 0.001% of the initial concentration in the water.

Fig. 2 compares the peaks in generated particles for experiments performed with 25 or 50 drops of 147 nm PSL solution added to Milli-Q water (Panel A) and with various concentrations (5–50 drops) of 103 nm PSL in Milli-Q water (Panel B). It is

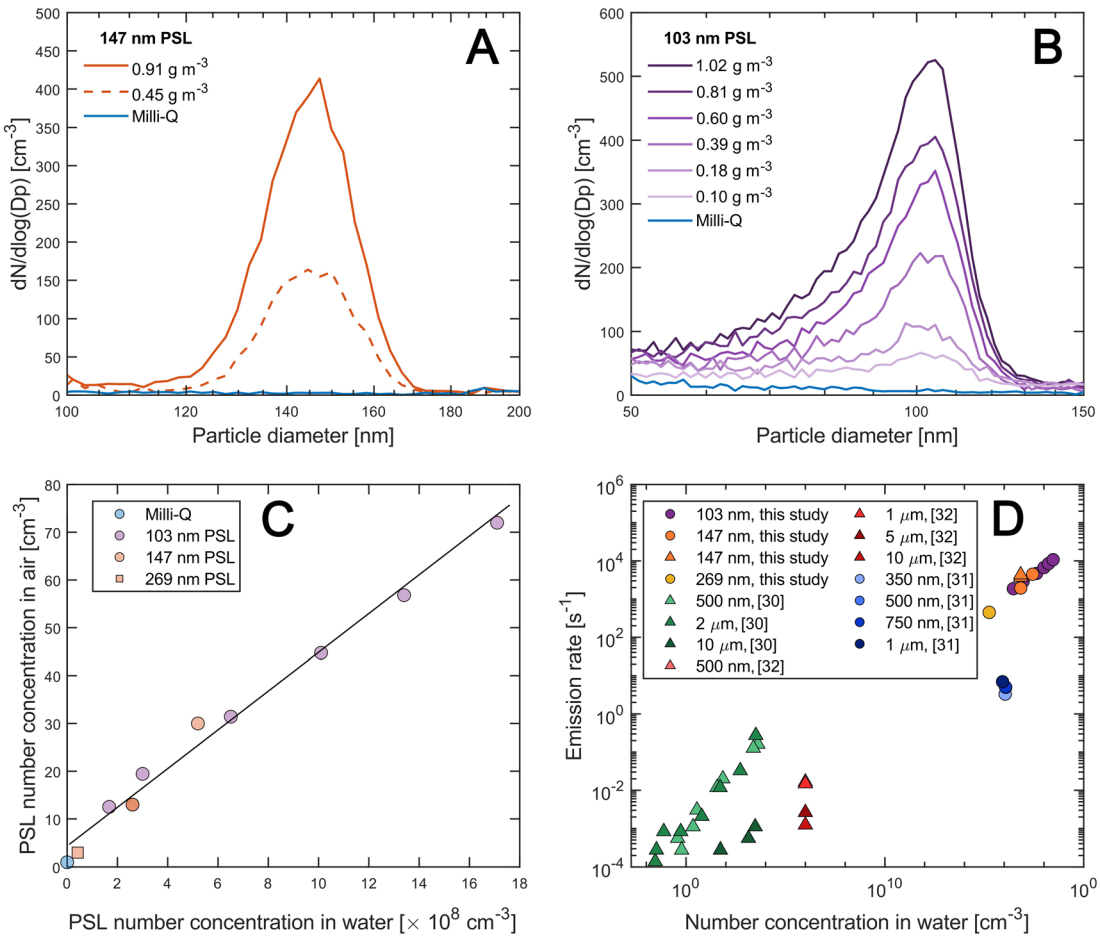

Fig. 2 Particle number generated in the AEGOR tank, as measured by the SMPS for a solution of 20 L Milli-Q water containing increasing concentrations of polystyrene latex (PSL). All data are averaged over 30 min (5 scans). (A) Particle number size distribution for 147 nm PSL (Experiment 1 and 2). (B) Particle number size distribution for 103 nm PSL (Experiment 6). (C) Number concentration in air (N_{air}) as a function of PSL concentration in water (N_w) including both 103, 147 and 269 nm PSL, experiments 1–4 and 6. Blue: integrated number concentration from Milli-Q water only (110–180 nm, Exp. 1), orange circles: 147 nm PSL, orange square: 269 nm PSL, purple circles: 103 nm PSL. Experiments were performed with a diffuser air flowrate of 3.35 L min^{-1} and at a constant temperature of 20 °C. A linear fit to the data gives $N_{air} = 4.0 \times 10^{-8} \times N_w + 3.9 \times cm^{-3}$. (D) Emission rate of polystyrene nanoplastic transfer to air *vs.* number concentration of nanoplastics in water for experiments from this study ($Q_{headspace}$ = 8.95 L min^{-1}, fresh water, diffuser) combined with results from Harb *et al.*[30] ($Q_{headspace}$ = 6 L min^{-1}, salinity 35 g kg^{-1}, plunging sheet), Oehlschlägel *et al.*[31] ($Q_{headspace}$ = 1.2 L min^{-1}, salinity 0 g kg^{-1}, diffuser) and Catarino *et al.*[32] ($Q_{headspace}$ = 10 L min^{-1}, salinity 31 g kg^{-1}, intermittent plunging jet). Both axes are on a logarithmic scale. Circles represent pure water experiments and triangles represent experiments from saline water. Catarino *et al.* report the number of particles captured on a filter that was sampled over 24 hours with a constant flowrate of air through the filter of 10 L min^{-1}. Based on this information we have estimated the number of particles per volume of air and the emission rate.

seen that increasing the concentration of PSL particles in the water increases the number of particles transferred from water to air for the same air flow rate through the diffuser. Fig. 2C compares the number concentration of airborne PSL particles (103, 147 or 269 nm) for different number concentrations of the PSL nanoparticles in water, suggesting that an approximately linear relationship exists between the concentration of nanoplastic particles in water (sizes 103–269 nm) and the number of nanoplastic particles transferred to air *via* bubble bursting for a fixed bubble flow rate. Harb *et al.*[30] recently reported a linear relationship on a logarithmic scale between the concentration of polystyrene spheres (0.5–10 μm) in air relative to artificial seawater.

Comparing plastic particle transfer from water to air measured in different laboratory systems is difficult because several metrics for comparison are specific to the individual setups. Harb *et al.*[30] report aerosolization factors for their experiments defined as the air to water concentration ratio ($[NP]_{air}/[NP]_{water}$) in the range 1.6×10^{-5}–2.4×10^{-7} increasing with decreasing size for polystyrene particles in salt water (35 g kg^{-1}). From the data given in Catarino *et al.*[32] we derive aerosolization factors in the range 7.4×10^{-9}–9.9×10^{-8} for polystyrene particles with diameters in the range of 0.5–5 μm. For our system the slope of the linear regression line in Fig. 2C corresponds to an aerosolization factor of 4.0×10^{-8} which is in agreement with data by Catarino *et al.* We speculate this could be consistent with an effect of salt in the water increasing the transfer of PS particles, see further discussion of the effect of salt below. Aerosolization factors are useful for comparing results of experiments in the same setup and between experimental setups with similar flow rate through the headspace (as the measured $[N_{air}]$ depends on the flow rate of air through the headspace). For the three studies mentioned above air flow through the headspace was 8.95 L min^{-1} (this study), 6 L min^{-1} (Harb *et al.*[30]) and 10 L min^{-1} (Catarino *et al.*[32]).

To place the results from this work in perspective, Fig. 2D shows emission rates *versus* the number concentrations in water observed in this study and in literature studies from which such information could be extracted. Emission rates were calculated as $N_{flux} = N_{air} \times Q_{headspace}$ following Harb *et al.*[30] and are given in Table 2. It should be kept in mind that the studies represented in Fig. 2D vary significantly in several ways. While the results of Harb *et al.*[30] and Catarino *et al.*[32] were performed in artificial sea water, our work and that of Oehlschlägel *et al.*[31] was performed in Milli-Q water. Furthermore, the studies herein and those of Oehlschlägel *et al.*[31] are based on measurements using a diffuser with a certain bubble flow rate and that for bubbling through saline water diffusers are known to produce different bubble size distributions and modes of particles than a plunging jet.[48,49] Even with these experimental differences, it is remarkable that across several orders of magnitude an increase in the number concentration of PS particles (size 0.1–10 μm) in water seems to suggest a monotonic increase in transfer to the air. The difference in emission rate at number concentrations in water between the results of this study and those of Oehlschlägel *et al.*[31] can in part be explained by the different diffuser flow rates (3.35 *vs.* 0.02 L min^{-1}, respectively). If the emission rate is normalized to the volume of air rising as bubbles per time the values for the number of particles emitted per volume of air entrained becomes of the same order of magnitude. Thus, while the figure should not be over-interpreted, it calls for future studies addressing the influence of particle number concentrations in water over the wide range of potential nanoplastic particle concentrations in seawater as well as freshwater under different conditions of for example bubble generation and air entrainment rate.

Fig. 3A shows how varying diffuser flow rates affect the particle size distribution sampled from the headspace of AEGOR for a solution of 147 nm PSL particles in Milli-Q water (Experiment 3). This figure illustrates that transfer of polystyrene particles from water to air depends on the bubble formation rate. Increasing the bubble formation rate through the diffuser increases particle production. This is consistent with results of Shiu *et al.*,[33] who show an increase in water to air transfer for micrometer-sized polystyrene particles with increasing diffuser flowrate (from 0.85 to 1 L min^{-1}). Oehlschlägel *et al.*[31] also observe an increase in airborne polystyrene particle number concentration for increasing flowrates of air through the water (0.01–0.02 L min^{-1}). For seawater Christiansen *et al.*[38] observed a linear relationship between generated sea salt aerosol and volume flow rate of air through the diffuser for flow rates up to 1.3 L min^{-1}. Sofieva *et al.*[47] performed similar experiments with a diffuser (NaCl solution) and observe an almost constant total number concentration with increasing flow rate for low flow rates (below 1 L min^{-1}) and a strong non-linear increase at higher flow rates (up to 2 L min^{-1}). Fig. 3B shows that in this work we are in a non-linear regime and the PSL particle number concentration in the headspace increases exponentially with the flow rate through the diffuser over the studied range of flow rates. We speculate that coalescence of air bubbles in the water column at high air flow rate in the diffuser could be a reason behind this

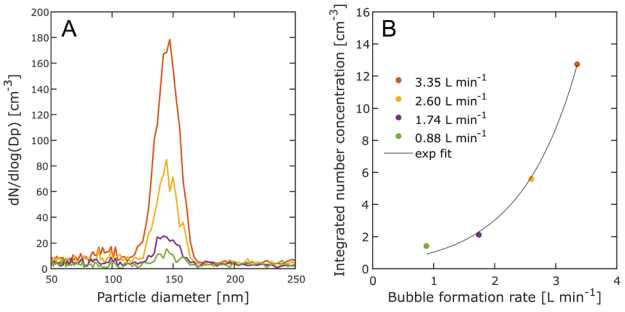

Fig. 3 (A) Mean particle number size distribution measured by the SMPS for a solution of 25 drops of 147 nm polystyrene latex (PSL) added to Milli-Q water in AEGOR (Experiment 3). Particles were produced with a diffuser with varying flow rates between 0.88 L min^{-1} to 3.35 L min^{-1}. An average over 48 min (8 scans) is shown. (B) Integrated number concentration over the region 110–180 nm with the same color-code as in panel A, determined by integrating a single log-normal distribution fit to dN/dlog (D_p) *vs.* D_p. The line is an exponential fit to the data.

observation along with reduction of the bubble lifetime with increasing air flow rate as suggested by Sofieva *et al.*[47]

Transfer of nanoplastics from saltwater

Fig. 4 shows the particle size distribution sampled from the headspace of AEGOR when bubbling air through a saltwater solution with varying salinities and containing 147 nm PSL particles (Experiment 5). The PSL particles show up as a peak at ~147 nm as seen in the pure water experiments. The salt particles create a peak at smaller diameters which grows to larger sizes with increasing salinity (see Fig. S10†). The plastic peak is clearly distinguishable from the salt peak until the salinity reaches 0.1 g kg^{-1}. The plastic signal is visible as a shoulder on the salt peak for the measurement with 0.2 g kg^{-1} of salinity. At higher salinities the salt peak broadens, engulfing the plastic peak.

To account for the influence of the salt peak the number concentration of nanoplastic in air was derived by fitting a sum of two log-normal distributions to the size spectra (see ESI Section S2† for details, here also upper number concentration limits based on single log-normal fits are given).

As seen from Table 2, our experiments suggest that the production flux of PSL particles is larger in Milli-Q water containing a small amount of salt (0.01–0.1 g kg^{-1}) than in pure Milli-Q water. This is consistent with observations by Shiu *et al.*[33] of higher transfer of micrometer sized polystyrene particles from medium (17 psu) and high (35 psu) salinity water than from pure water. There could be several factors contributing to the effect of even small amounts of salt on PSL transfer from water to air. It is known that ions in sea salt diminish bubble coalescence. This results in a higher proportion of smaller bubbles in salt water compared to fresh water[42,50,51] and a difference in surface bubble coverage and lifetime.[50,52]

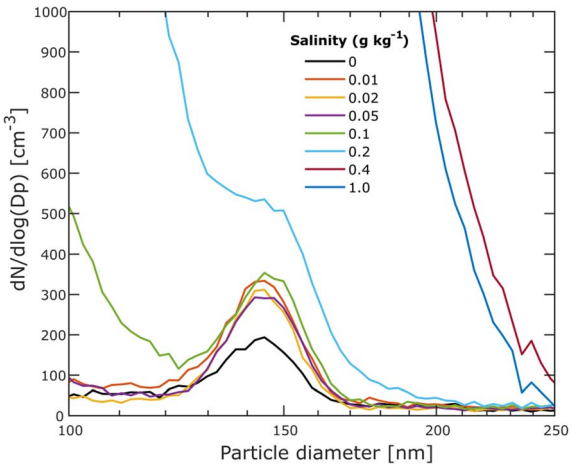

Fig. 4 Mean particle number size distribution in air measured by the SMPS for a solution of 20 L Milli-Q water containing 25 drops of 147 nm PSL and varying salinity of synthetic sea salt (figure centered on the PSL peak). The diffuser flow rate was 3.35 L min^{-1} and temperature was held at 20 °C (Experiment 5). All data are an average of 78 min (13 scans). The full spectrum is shown in Fig. S10.†

Mårtensson *et al.*[53] report an order of magnitude increase in salt particle number concentration from 0.9 g kg^{-1} to 3 g kg^{-1} salinity. Zinke *et al.*[54] show that salt particle production from saline water increases with increasing salinity in a non-linear way with the highest increase in particle production per salinity unit for salinities smaller than 5 g kg^{-1}. Zinke *et al.*[54] relates this to a transition in bubble coalescence with salinity. Recently, Dubitsky *et al.*[55] showed experimental evidence suggesting that salinity affects sub-micron aerosol production by affecting the length scale of the bursting bubble film across different salts, bubble coalescence and bubble generation mechanisms. While the mechanism is not clear we speculate that there could be a link between the potential effect of salt on underwater bubble size distribution, bubble surface lifetime and bubble film thickness and the transfer of polystyrene nanoplastic to air *via* bubble bursting.

Conclusions

This study demonstrates and quantifies transfer of nanoplastic PSL particles (<300 nm) from water to air *via* bubbles bursting and suggests that small amounts of salt increases polystyrene particle emission. We find that the transfer depends on bubble formation rate and scales linearly with the number concentration of plastic particles in water at concentrations likely corresponding to highly polluted areas.

This complements existing data suggesting a similar trend at low concentrations and reveals an increasing trend in plastic particle transfer from water to air over the entire range of current estimates of plastic particle concentrations in surface waters. In this work bubbles were generated using a diffuser at the bottom of the AEGOR sea spray simulation tank in line with several other studies targeting water–air transfer of microplastics.[31,33,34] It is known that the size distribution of sea spray aerosol generated from the diffuser is narrower than the size distribution obtained when air is entrained *via* a plunging jet in AEGOR.[38] Thus, in future studies it would be interesting and relevant to probe nanoplastic particle transfer using the plunging jet at different velocities corresponding to different air entrainment rates. This work is thus expected to contribute to the growing understanding of plastic polluted surface waters as sources of airborne nanoplastics. Future studies should address transfer of other types, sizes and concentrations of plastic polymer particles from water to air and include in a systematic way more complex freshwater proxies. Additionally, salinity seems to play an important role which should be further investigated. Recent studies suggest a strong effect of temperature on sea spray aerosol production.[47,54] and the effect of temperature on transfer of nanoplastic from water to air clearly warrants future study.

Author contributions

Eva R. Kjærgaard: investigation, methodology, data curation, formal analysis, visualization, writing – original draft, writing – review & editing. Freja Hasager: investigation, methodology, writing – review & editing. Sarah S. Petters: investigation,

methodology, writing – review & editing. Marianne Glasius: conceptualization, methodology, supervision, funding acquisition, writing – review & editing. Merete Bilde: conceptualization, methodology, writing – review & editing, supervision, project administration, funding acquisition.

Conflicts of interest

There are no conflicts to declare.

Acknowledgements

The authors thank Lærke Sloth Nielsen for assisting with SMPS transfer function calculations, Mads Mørk Jensen for technical assistance and Bernadette Rosati for discussions. We thank Hosein Foroutan for providing data from Harb *et al.*[30] used in Fig. 2D. We acknowledge the Independent Research Fund Denmark (grant number 0217-00442B) and the Danish National Research Foundation (DNRF172) through the Center of Excellence for Chemistry of Clouds for funding.

References

1 D. Allen, S. Allen, S. Abbasi, A. Baker, M. Bergmann, J. Brahney, *et al.*, Microplastics and nanoplastics in the marine-atmosphere environment, *Nat. Rev. Earth Environ.*, 2022, **3**(6), 393–405.
2 J. Zalasiewicz, C. N. Waters, J. A. Ivar do Sul, P. L. Corcoran, A. D. Barnosky, A. Cearreta, *et al.*, The geological cycle of plastics and their use as a stratigraphic indicator of the Anthropocene, *Anthropocene*, 2016, **13**, 4–17.
3 F. Corradini, P. Meza, R. Eguiluz, F. Casado, E. Huerta-Lwanga and V. Geissen, Evidence of microplastic accumulation in agricultural soils from sewage sludge disposal, *Nat. Rev. Earth Environ.*, 2019, **671**, 411–420.
4 S.-A. Strungaru, R. Jijie, M. Nicoara, G. Plavan and C. Faggio, Micro- (nano) plastics in freshwater ecosystems: Abundance, toxicological impact and quantification methodology, *TrAC, Trends Anal. Chem.*, 2019, **110**, 116–128.
5 M. A. Browne, Sources and Pathways of Microplastics to Habitats, *Marine Anthropogenic Litter*, Cham, Springer International Publishing, 2015. pp. 229–244.
6 B. Baensch-Baltruschat, B. Kocher, F. Stock and G. Reifferscheid, Tyre and road wear particles (TRWP) - A review of generation, properties, emissions, human health risk, ecotoxicity, and fate in the environment, *Nat. Rev. Earth Environ.*, 2020, **733**, 137823.
7 S. Allen, D. Allen, F. Baladima, V. R. Phoenix, J. L. Thomas, G. Le Roux, *et al.*, Evidence of free tropospheric and long-range transport of microplastic at Pic du Midi Observatory, *Nat. Commun.*, 2021, **12**(1), 7242.
8 N. Evangeliou, H. Grythe, Z. Klimont, C. Heyes, S. Eckhardt, S. Lopez-Aparicio, *et al.*, Atmospheric transport is a major pathway of microplastics to remote regions, *Nat. Commun.*, 2020, **11**(1), 3381.
9 F. Hasager, P. N. Björgvinsdóttir, S. F. Vinther, A. Christofili, E. R. Kjærgaard, S. S. Petters, *et al.*, Development and validation of an analytical pyrolysis method for detection of airborne polystyrene nanoparticles, *J. Chromatogr. A*, 2024, **1717**, 464622.
10 S. S. Petters, E. R. Kjærgaard, F. Hasager, A. Massling, M. Glasius and M. Bilde, Morphology and hygroscopicity of nanoplastics in sea spray, *Phys. Chem. Chem. Phys.*, 2023, **25**, 32430–32442.
11 Y. Chen, S. Jing, Y. Wang, Z. Song, L. Xie, X. Shang, *et al.*, Quantification and Characterization of Fine Plastic Particles as Considerable Components in Atmospheric Fine Particles, *Environ. Sci. Technol.*, 2024, **58**(10), 4691–4703.
12 S. Niu, R. Liu, Q. Zhao, S. Gagan, A. Dodero, Q. Ying, *et al.*, Quantifying the Chemical Composition and Real-Time Mass Loading of Nanoplastic Particles in the Atmosphere Using Aerosol Mass Spectrometry, *Environ. Sci. Technol.*, 2024, **58**(7), 3363–3374.
13 L. F. Amato-Lourenço, L. dos Santos Galvão, L. A. de Weger, P. S. Hiemstra, M. G. Vijver and T. Mauad, An emerging class of air pollutants: Potential effects of microplastics to respiratory human health?, *Nat. Rev. Earth Environ.*, 2020, **749**, 141676.
14 S. Allen, D. Allen, K. Moss, G. Le Roux, V. R. Phoenix and J. E. Sonke, Examination of the ocean as a source for atmospheric microplastics, *PLoS One*, 2020, **15**(5), e0232746.
15 M. Ganguly and P. A. Ariya, Ice Nucleation of Model Nanoplastics and Microplastics: A Novel Synthetic Protocol and the Influence of Particle Capping at Diverse Atmospheric Environments, *ACS Earth Space Chem.*, 2019, **3**(9), 1729–1739.
16 L. E. Revell, P. Kuma, E. C. Le Ru, W. R. C. Somerville and S. Gaw, Direct radiative effects of airborne microplastics, *Nature*, 2021, **598**(7881), 462–467.
17 M. Trainic, J. M. Flores, I. Pinkas, M. L. Pedrotti, F. Lombard, G. Bourdin, *et al.*, Airborne microplastic particles detected in the remote marine atmosphere, *Commun. Earth Environ.*, 2020, **1**(1), 64.
18 S. Yang, T. Zhang, Y. Gan, X. Lu, H. Chen, J. Chen, *et al.*, Constraining Microplastic Particle Emission Flux from the Ocean, *Environ. Sci. Technol. Lett.*, 2022, **9**(6), 513–519.
19 J. Brahney, N. Mahowald, M. Prank, G. Cornwell, Z. Klimont, H. Matsui, *et al.*, Constraining the atmospheric limb of the plastic cycle, *Proc. Natl. Acad. Sci. U. S. A.*, 2021, **118**(16), e2020719118.
20 A. J. Tanentzap, S. Cottingham, J. Fonvielle, I. Riley, L. M. Walker, S. G. Woodman, *et al.*, Microplastics and anthropogenic fibre concentrations in lakes reflect surrounding land use, *PLoS Biol.*, 2021, **19**(9), e3001389.
21 V. Nava, S. Chandra, J. Aherne, M. B. Alfonso, A. M. Antão-Geraldes, K. Attermeyer, *et al.*, Plastic debris in lakes and reservoirs, *Nature*, 2023, **619**(7969), 317–322.
22 N. W. May, M. J. Gunsch, N. E. Olson, A. L. Bondy, R. M. Kirpes, S. B. Bertman, *et al.*, Unexpected Contributions of Sea Spray and Lake Spray Aerosol to Inland Particulate Matter, *Environ. Sci. Technol. Lett.*, 2018, **5**(7), 405–412.

23 E. van Sebille, C. Wilcox, L. Lebreton, N. Maximenko, B. D. Hardesty, J. A. van Franeker, *et al.*, A global inventory of small floating plastic debris, *Environ. Res. Lett.*, 2015, **10**(12), 124006.
24 W. Courtene-Jones, S. van Gennip, J. Penicaud, E. Penn and R. C. Thompson, Synthetic microplastic abundance and composition along a longitudinal gradient traversing the subtropical gyre in the North Atlantic Ocean, *Mar. Pollut. Bull.*, 2022, **185**, 114371.
25 D. Materić, R. Holzinger and H. Niemann, Nanoplastics and ultrafine microplastic in the Dutch Wadden Sea – The hidden plastics debris?, *Nat. Rev. Earth Environ.*, 2022, **846**, 157371.
26 R. Egessa, A. Nankabirwa, H. Ocaya and W. G. Pabire, Microplastic pollution in surface water of Lake Victoria, *Nat. Rev. Earth Environ.*, 2020, 7**41**, 140201.
27 W. Wang, W. Yuan, Y. Chen and J. Wang, Microplastics in surface waters of Dongting Lake and Hong Lake, China, *Nat. Rev. Earth Environ.*, 2018, **633**, 539–545.
28 L. Su, Y. Xue, L. Li, D. Yang, P. Kolandhasamy, D. Li, *et al.*, Microplastics in Taihu Lake, China, *Environ. Pollut.*, 2016, **216**, 711–719.
29 S. A. Mason, L. Kammin, M. Eriksen, G. Aleid, S. Wilson, C. Box, *et al.*, Pelagic plastic pollution within the surface waters of Lake Michigan, USA, *J. Great Lakes Res.*, 2016, **42**(4), 753–759.
30 C. Harb, N. Pokhrel and H. Foroutan, Quantification of the Emission of Atmospheric Microplastics and Nanoplastics via Sea Spray, *Environ. Sci. Technol. Lett.*, 2023, **10**(6), 513–519.
31 L. M. Oehlschlägel, S. Schmid, M. Lehmann, S. Gekle and A. Held, Water–air transfer rates of microplastic particles through bubble bursting as a function of particle size, *Microplast. nanoplast.*, 2024, **4**(1), 1.
32 A. I. Catarino, M. C. León, Y. Li, S. Lambert, M. Vercauteren, J. Asselman, *et al.*, Micro- and nanoplastics transfer from seawater to the atmosphere through aerosolization under controlled laboratory conditions, *Mar. Pollut. Bull.*, 2023, **192**, 115015.
33 R.-F. Shiu, L.-Y. Chen, H.-J. Lee, G.-C. Gong and C. Lee, New insights into the role of marine plastic-gels in microplastic transfer from water to the atmosphere via bubble bursting, *Water Res.*, 2022, **222**, 118856.
34 M. Masry, S. Rossignol, B. Temime Roussel, D. Bourgogne, P.-O. Bussière, B. R'mili, *et al.*, Experimental evidence of plastic particles transfer at the water-air interface through bubble bursting, *Environ. Pollut.*, 2021, **280**, 116949.
35 D. B. Shaw, Q. Li, J. K. Nunes and L. Deike, Ocean emission of microplastic, *PNAS Nexus*, 2023, **2**(10), pgad296.
36 R. Geyer, J. R. Jambeck and K. L. Law, Production, use, and fate of all plastics ever made, *Sci. Adv.*, 2017, **3**(7), e1700782.
37 A. L. Andrady, Microplastics in the marine environment, *Mar. Pollut. Bull.*, 2011, **62**(8), 1596–1605.
38 S. Christiansen, M. E. Salter, E. Gorokhova, Q. T. Nguyen and M. Bilde, Sea Spray Aerosol Formation: Laboratory Results on the Role of Air Entrainment, Water Temperature, and Phytoplankton Biomass, *Environ. Sci. Technol.*, 2019, **53**(22), 13107–13116.
39 G. de Leeuw, E. L. Andreas, M. D. Anguelova, C. W. Fairall, E. R. Lewis, C. O'Dowd, *et al.*, Production flux of sea spray aerosol, *Rev. Geophys.*, 2011, **49**(2), RG2001.
40 P. K. Quinn, D. B. Collins, V. H. Grassian, K. A. Prather and T. S. Bates, Chemistry and Related Properties of Freshly Emitted Sea Spray Aerosol, *Chem. Rev.*, 2015, **115**(10), 4383–4399.
41 C. Harb and H. Foroutan, Experimental development of a lake spray source function and its model implementation for Great Lakes surface emissions, *Atmos. Chem. Phys.*, 2022, **22**(17), 11759–11779.
42 N. W. May, J. L. Axson, A. Watson, K. A. Pratt and A. P. Ault, Lake spray aerosol generation: a method for producing representative particles from freshwater wave breaking, *Atmos. Meas. Tech.*, 2016, **9**(9), 4311–4325.
43 L. S. Nielsen and M. Bilde, Exploring controlling factors for sea spray aerosol production: temperature, inorganic ions and organic surfactants, *Tellus B*, 2020, **72**(1), 1–10.
44 I. N. Tang, A. C. Tridico and K. H. Fung, Thermodynamic and optical properties of sea salt aerosols, *J. Geophys. Res.: Atmos.*, 1997, **102**(D19), 23269–23275.
45 P. Zieger, O. Väisänen, J. C. Corbin, D. G. Partridge, S. Bastelberger, M. Mousavi-Fard, *et al.*, Revising the hygroscopicity of inorganic sea salt particles, *Nat. Commun.*, 2017, **8**(1), 15883.
46 M. E. Salter, E. D. Nilsson, A. Butcher and M. Bilde, On the seawater temperature dependence of the sea spray aerosol generated by a continuous plunging jet, *J. Geophys. Res.: Atmos.*, 2014, **119**(14), 9052–9072.
47 S. Sofieva, E. Asmi, N. S. Atanasova, A. E. Heikkinen, E. Vidal, J. Duplissy, *et al.*, Effects of temperature and salinity on bubble-bursting aerosol formation simulated with a bubble-generating chamber, *Atmos. Meas. Tech.*, 2022, **15**(20), 6201–6219.
48 E. Fuentes, H. Coe, D. Green, G. de Leeuw and G. McFiggans, Laboratory-generated primary marine aerosol via bubble-bursting and atomization, *Atmos. Meas. Tech.*, 2010, **3**(1), 141–162.
49 M. D. Stokes, G. B. Deane, K. Prather, T. H. Bertram, M. J. Ruppel, O. S. Ryder, *et al.*, A Marine Aerosol Reference Tank system as a breaking wave analogue for the production of foam and sea-spray aerosols, *Atmos. Meas. Tech.*, 2013, **6**(4), 1085–1094.
50 E. C. Monahan and C. R. Zietlow, Laboratory comparisons of fresh-water and salt-water whitecaps, *J. Geophys. Res.*, 1969, **74**(28), 6961–6966.
51 W. M. Carey, J. W. Fitzgerald, E. C. Monahan and Q. Wang, Measurement of the sound produced by a tipping trough with fresh and salt water, *J. Acoust. Soc. Am.*, 1993, **93**(6), 3178–3192.
52 C. Harb and H. Foroutan, A systematic analysis of the salinity effect on air bubbles evolution: Laboratory

experiments in a breaking wave analog, *J. Geophys. Res.: Oceans*, 2019, **124**(11), 7355–7374.

53 E. M. Mårtensson, E. D. Nilsson, G. de Leeuw, L. H. Cohen and H.-C. Hansson, Laboratory simulations and parameterization of the primary marine aerosol production, *J. Geophys. Res.: Atmos.*, 2003, **108**(D9), 4297.

54 J. Zinke, E. D. Nilsson, P. Zieger and M. E. Salter, The Effect of Seawater Salinity and Seawater Temperature on Sea Salt Aerosol Production, *J. Geophys. Res.: Atmos.*, 2022, **127**(16), e2021JD036005.

55 L. Dubitsky, M. D. Stokes, G. B. Deane and J. C. Bird, Effects of Salinity Beyond Coalescence on Submicron Aerosol Distributions, *J. Geophys. Res.: Atmos.*, 2023, **128**(10), e2022JD038222.